Heterogeneous and homogeneous photocatalytic degradation of the insecticide imidacloprid in aqueous solutions

V. Kitsiou [a], N. Filippidis [a], D. Mantzavinos [b], I. Poulios [a,*]

[a] Laboratory of Physical Chemistry, Department of Chemistry, Aristotle University of Thessaloniki, GR-54124 Thessaloniki, Greece
[b] Department of Environmental Engineering, Technical University of Crete, Polytechneioupolis, GR-73100 Chania, Greece

ARTICLE INFO

ABSTRACT

The heterogeneous and homogeneous photocatalytic degradation of imidacloprid, a systemic chloronicotinoid insecticide, has been investigated in aqueous solutions using artificial UV-A or visible illumination. Three processes under various experimental conditions were evaluated namely, TiO_2/UV-A, photo-Fenton/UV-A and photo-Fenton/vis with respect to their activity for substrate degradation and mineralization. The initial apparent photonic efficiency decreased in the order photo-Fenton/UV-A > TiO_2/UV-A > photo-Fenton/vis. For the TiO_2/UV-A process, the efficiency increased considerably when TiO_2 is combined with Fe^{3+} and H_2O_2 presumably due to the synergistic effect of homogeneous and heterogeneous photocatalytic reaction. On the other hand, the homogeneous photocatalytic reactions were enhanced in the presence of the oxalate ions. Imidacloprid degradation was accompanied by the formation of several reaction by-products as confirmed by GC/MS analysis, while ammonium, nitrate and chloride ions have been detected in the liquid phase as mineralization products. By-products were less ecotoxic to marine bacteria than the insecticide itself.

© 2008 Published by Elsevier B.V.

1. Introduction

Research devoted to environmental protection has been developed rather quickly as a consequence of the special attention paid to the environment by international, social, and political authorities [1] leading, in some cases, to severe environmental regulations [2]. Strict quality standards exist in the case of toxic substances that affect the balance and the proper function of the ecosystem. Among these substances, pesticides represent one of the greatest problems, because as the world population increases, the necessity to increase agricultural productivity will become inevitable. This fact will lead to an even greater rise of the production and consumption of agrochemical products.

Pesticides and agrochemical compounds in general have been detected in water since the 1950s. The United Nations estimate that less than 1% of all pesticides used in agriculture actually reach the crops. The remaining contaminates the land, the air and particularly the water [3–5]. As these contaminants are in many cases toxic and non-biodegradable, they tend to accumulate in the environment with unpredictable consequences for the mid-term future [6]. An ideal treatment method for pesticide wastes would be a non-selective one that could achieve rapid and complete degradation to inorganic products and could be suitable for small-scale treatment units [7].

Treatment methods currently employed for agrochemicals degradation include advanced chemical oxidation, adsorption on granular activated carbon and incineration. Among the so-called advanced oxidation processes (AOPs), photocatalytic methods, in the presence of artificial or solar light, like heterogeneous photocatalysis (TiO_2/UV-A) or the photo-Fenton reagent (Fe^{3+}/H_2O_2/UV-A or vis) have been proven to be effective for the degradation of various contaminants found in industrial or domestic wastewaters [7–9]. A variety of toxic agrochemical substances, such as insecticides and pesticides, have been also studied in regard to their photocatalytic degradation, in the presence of artificial or solar illumination, with very encouraging results, while studies dealing with real or simulated wastewater have revealed that their complete or partial degradation is possible via the above mentioned methods [7,9–13].

Our present study describes the photocatalytic decomposition and mineralization of imidacloprid a systemic chloronicotinoid insecticide, using heterogeneous photocatalysis with TiO_2 powder in suspension and homogeneous photocatalysis with the photo-Fenton and ferrioxalate reagents in order to assess the effect of

various operating conditions on pesticide degradation, mineralization and ecotoxicity. Major degradation by-products were also determined.

Imidacloprid belongs to a new class of insecticides, called neonicotinoids. Since its launch in 1991, products containing imidacloprid have gained registrations in about 120 countries and are marketed for use in agriculture (for over 140 agricultural crops), on turf, pets and for household pests [14]. Imidacloprid acts as an agonist on the postsynaptic nicotinic acetylcholine receptors of motor neurones in insects. This causes an overstimulation of the nervous system, and ultimately kills the insect [15].

2. Experimental and analytical

2.1. Chemicals

Imidacloprid, 1-[(6-chloro-3-pyridinyl)methyl]-N-nitro-2-imidazolidinimine, technical grade (99% purity), whose structure is shown in Fig. 8, was purchased from the company FarmaChem, Thessaloniki, Greece.

Heterogeneous photocatalytic tests were carried out using TiO_2 P-25 Degussa Huells (anatase/rutile: 3.6/1, surface area 56 $m^2\,g^{-1}$, nonporous), ZnO (Merck, BET 10 $m^2\,g^{-1}$) and TiO_2 UV100 (anatase 250 $m^2\,g^{-1}$) from Schachtleben Chemie GmbH. $HClO_4$ from Merck was used to adjust the pH when necessary. Iron (III) chloride ($FeCl_3\cdot 6H_2O$), hydrogen peroxide (30%) and all other chemicals for the experiments with the photo-Fenton and ferrioxalate reagents were purchased from Fluka Chemie and used without further purification. Doubly distilled water was used throughout the work. Aqueous stock solutions of imidacloprid (200 mg L^{-1}) were prepared every week, protected from light and stored at 25 °C.

2.2. Experimental setup and procedures

Experiments were performed in an thermostated Pyrex cell of 600 mL capacity (6.6 cm diameter, 11 cm height). The reaction vessel was fitted with either a UV-A or vis central 9W lamp of identical dimensions and geometry and had inlet and outlet ports for sparging the desired gas under which the reaction took place. The spectral response of the UV-A irradiation source (Radium Ralutec 9W/78), according to the manufacturer, ranged between 340 and 400 nm with a maximum at 366 nm. The spectral response of the visible irradiation source (Radium Ralutec 9W/71), with exact the same geometry as the previous one, ranged between 400 and 550 nm with a maximum at 440 nm. The photon flow per unit volume of the incident light was determined using chemical actinometry with potassium ferrioxalate [16]. The initial light intensity under exactly the same conditions as in the photocatalytic experiments, was measured at 1.039×10^{-4} einstein min^{-1} in the case of UV-A and 0.606×10^{-4} einstein min^{-1} in the case of visible irradiation.

During the photocatalytic experiments, 500 mL of the imidacloprid solution containing the appropriate quantity of the semiconductor powder or the photo-Fenton reagents was magnetically stirred, while the solution was purged continuously with CO_2-free air. At specific time intervals samples of 6 mL were withdrawn, filtered through a 0.45 μm filter (Schleicher and Schuell) in order to remove TiO_2 particles (in the case of heterogeneous photocatalysis) and subsequently analyzed.

Heterogeneous photocatalytic experiments with TiO_2 were carried out at the suspension's natural pH which was 5.2, unless otherwise stated in the text. For the runs with ZnO, the initial pH value of the suspension was 7.2 due to the basic nature of the catalyst. Homogeneous runs were performed at pH 3.2, thus avoiding precipitation of Fe^{3+}.

The reaction temperature was kept constant at 25 ± 1 °C. Some photocatalytic experiments were repeated three times in order to check the reproducibility of the experimental results. The accuracy of the optical density values was within ±5%, while the corresponding ones of DOC, inorganic ions and toxicity were within ±10%.

2.3. Analytical methods

Changes in the concentration of imidacloprid were followed by its characteristic absorbance at 270 nm using a UV–vis spectrophotometer (Shimadzu UV-1700). Since a linear dependence between the initial concentration of the pesticide and the absorbance at 270 nm was found to occur, its decomposition was monitored spectrophotometrically at this wavelength.

In order to determine the extent of mineralization, dissolved organic carbon (DOC) was measured using a Schimadzu V_{CSH} TOC Analyzer, while the inorganic ions released in the liquid phase following the oxidative conversion of imidacloprid were detected using a Dionex 4500i Ion Analyzer (Dionex, CA, USA) equipped with cation and anion micromembrane suppressors and a pulsed electrical conductivity detector.

GC/MS analysis was employed to identify reaction by-products from photocatalytic degradation. Prior to GC/MS analysis, the samples were pre-concentrated using two different techniques, namely (i) solid-phase microextraction (SPME) and (ii) acid extraction in an attempt to identify as many by-products as possible. Immersion SPME with a polydimethylsiloxane (PDMS) fibre was employed to pre-concentrate the samples, while separation of the extracted compounds was carried out on a Shimadzu GC-17A QP-5050A GC/MS system equipped with a 30 m × 0.25 mm, 0.25 μm HP-5MS capillary column (Agilent Technologies); details of SPME procedures [17] and GC/MS operating conditions are given elsewhere [18]. Acid extraction involved acidification of 35 mL of sample at pH 2.5 with sulphuric acid, addition of 15 g anhydrous sodium sulphate and extraction with $3\times$ 15 mL ethyl acetate. The organic extracts were filtered through a thin layer of anhydrous sodium sulphate and concentrated in a rotary evaporator down to 2–3 mL. The remaining volume was evaporated to dryness with a gentle nitrogen stream and re-dissolved with sonication in 1 mL of cyclohexane:ethyl acetate (8:2). GC/MS analysis was performed on the same equipment used for SPME-treated samples according to the following conditions: the injector temperature was 270 °C and the column oven was initially set at 60 °C for 1 min, then programmed to 180 at a 25 °C min^{-1} rate and finally to 280 °C at a 5 °C min^{-1} rate, where it was held for 5 min. The interface temperature was set at 300 °C and the detector voltage at 1.4 kV. A solvent cut time of 4.5 min was selected to avoid detector saturation. The ionization mode was electron impact (70 eV) and data was collected from 50 to 300 m/z at 0.5 s scan interval.

The luminescent marine bacterium *Vibrio fischeri* was used to assess the acute ecotoxicity of imidacloprid samples prior to and after the photocatalytic treatment. The inhibition of bioluminescence of *V. fischeri* exposed to untreated and treated samples for 15 min at 15 °C was measured using a LUMIStox analyzer (Dr Lange, Germany) and the results were compared to an aqueous control with color correction. Test procedures are given in detail elsewhere [19].

2.4. Initial apparent photonic efficiency

The photonic efficiency (ζ) describing the effectiveness of light conversion to product in heterogeneous, light scattering systems, is directly proportional to the quantum yield, and may be considered to be the lower limit of this commonly used measure of light efficiency [20,21].

For imidacloprid photooxidation, the following equation was used to compute the initial apparent photonic efficiency:

$$\zeta_0\ (\%) = r_0(255.5 I_{hv} 10^3)^{-1} \times 100 \tag{1}$$

where r_0 is the initial reaction rate of the photooxidation ($\mathrm{mg\,L^{-1}\,min^{-1}}$), 255.5 is the molecular weight of imidacloprid and I_{hv} is the incident photon flux (mol photons $\mathrm{L^{-1}\,min^{-1}}$ = einstein $\mathrm{min^{-1}}$).

For mineralization, the initial apparent photonic efficiency, ζ_{DOC}, per carbon atom conversion can be calculated as follows

$$\zeta_{DOC}\ (\%) = r_{DOC}(12 I_{hv} 10^3)^{-1} \times 100 \tag{2}$$

where r_{DOC} is the initial rate of DOC reduction ($\mathrm{mg\,L^{-1}\,min^{-1}}$).

3. Results and discussion

3.1. Heterogeneous photocatalytic experiments

General description of the heterogeneous photocatalytic oxidation of organic pollutants in the presence of TiO_2 as catalyst under artificial or solar irradiation is presented in several excellent review articles [8,22,23]. A brief summary is presented here only for the sake of completeness.

It is well established, that by the irradiation of an aqueous TiO_2 suspension with light energy greater than the band gap energy of the semiconductor ($E_g > 3.2$ eV), conduction band electrons (e^-) and valence band holes (h^+) are generated. Part of the photogenerated carriers recombine in the bulk of the semiconductor, while the rest reach the surface, where the holes, as well as the electrons, act as powerful oxidants and reductants, respectively. The photogenerated electrons react with the adsorbed molecular O_2 on the Ti(III)-sites, reducing it to superoxide radical anion O_2^-, while the photogenerated holes can oxidize either the organic molecules directly, or the OH^- ions and the H_2O molecules adsorbed at the TiO_2 surface to $OH^\bullet$ radicals. These radicals together with other highly oxidant species (e.g. peroxide radicals) are reported to be responsible for the primary oxidizing step in photocatalysis. The $OH^\bullet$ radicals formed on the illuminated semiconductor surface are very strong oxidizing agents, with a standard reduction potential of 2.8 V. These can easily attack the adsorbed organic molecules or those located close to the surface of the catalyst, thus leading finally to their complete mineralization.

Screening experiments were performed to assess the catalytic activity of various semiconductors, namely TiO_2 P-25, TiO_2 UV-100 and ZnO. Fig. 1 shows concentration–time profiles during imidacloprid UV-A photocatalytic oxidation at 20 mg L^{-1} initial concentration and 0.5 g L^{-1} catalyst loading. As seen, reactivity decreases in the order ZnO > TiO_2 P-25 > TiO_2 UV-100, with the degradation efficiency after 60 min of illumination being 76, 64 and 26%, respectively. Although ZnO has similar band gab energy and band edge position to TiO_2, its nonstoichiometry leads to electron mobility of at least two orders of magnitude higher than TiO_2. This results in a quicker charge transfer with the various species in the solution and consequently to lower recombination rates in comparison to TiO_2 [24,25]. However, even though ZnO at pH 7.2 exhibited the best catalytic activity in the studied conditions, its application is limited by its corrosion and photocorrosion that may result in the increase of the toxicity of the solution. It is well known from the literature that below pH 9 a dissolution of ZnO takes place, which increases by illumination as a result of the attack of the Zn–O bonds by the photogenerated holes [26,27]. This leads to a release of Zn^{2+} ions into the suspension and
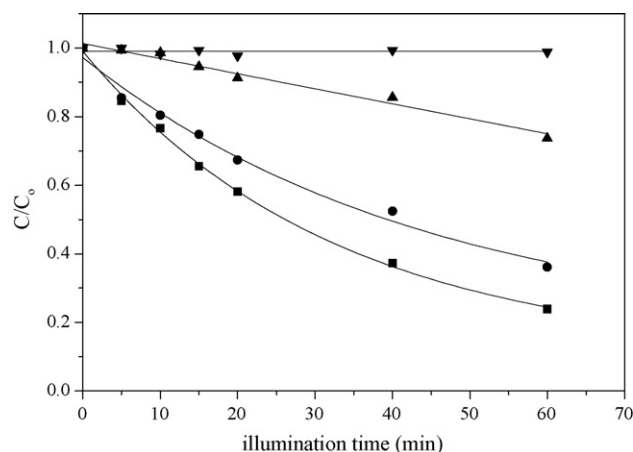

Fig. 1. Heterogeneous photocatalytic degradation of 20 mg L^{-1} imidacloprid as a function of illumination time in the presence of 0.5 g L^{-1} catalyst: (■) ZnO at pH 7.2, (●) TiO_2 P-25 at pH 5.2, (▲) TiO_2 UV-100 at pH 5.2, and (▼) without catalyst.

to an increase of the toxicity, taking into account that for the bacteria *V. fischeri* the EC_{50} for Zn^{2+} is 1.62 mg L^{-1} [28].

On the contrary, a very small decrease in the concentration of this compound was observed by illumination in the absence of any catalyst (Fig. 1). After 2 h of irradiation with UV-A light ($hv > 340$ nm), direct photolysis contributed less than 5% to the degradation of imidacloprid.

The photocatalytic degradation rate of organic compounds is commonly described by a pseudo-first order kinetic expression, which is rationalized in terms of the Langmuir–Hinshelwood model, modified to accommodate reactions occurring at the solid–liquid interface [29,30].

$$r_0 = -\frac{dC}{dt} = \frac{k_r K C_{eq}}{1 + K C_{eq}} \tag{3}$$

where r_0 is the initial rate of disappearance of the organic substrate and C_{eq} is the equilibrium bulk-solute concentration. K represents the equilibrium constant of adsorption of the organic substrate onto TiO_2 and k_r reflects the limiting rate constant of reaction at maximum coverage under the given experimental conditions. This equation can be used when data demonstrate linearity plotted as follows:

$$\frac{C_{eq}}{r_0} = \frac{1}{k_r K} + \frac{C_{eq}}{k_r} \tag{4}$$

The effect of altering the equilibrium concentration of imidacloprid on the initial reaction rate (r_0) of photodegradation is shown in Fig. 2. The curve is reminiscent of a Langmuir type isotherm, at which the rate value of decomposition first increases and then reaches a saturation value at high concentrations of imidacloprid. The r_0 values were independently obtained by a linear fit of the C_{eq}–t data in the range of 5–50 mg L^{-1} initial imidacloprid concentration. Only the experimental data obtained during the first 10 min illumination were used in calculating the initial reaction rates, in order to minimize variations as a result of the competitive effects of the intermediates, pH changes, etc. It is well known that the intermediate products formed during photodegradation furthermore undergo photocatalytic oxidation, while the simultaneous release of H^+ influences the pH of the solution, thus resulting in a change of the initial conditions. Due to the fact that imidacloprid is adsorbed quite strongly on the TiO_2 P-25 surface, the equilibrium concentration of the pesticide (C_{eq}), after 30 min
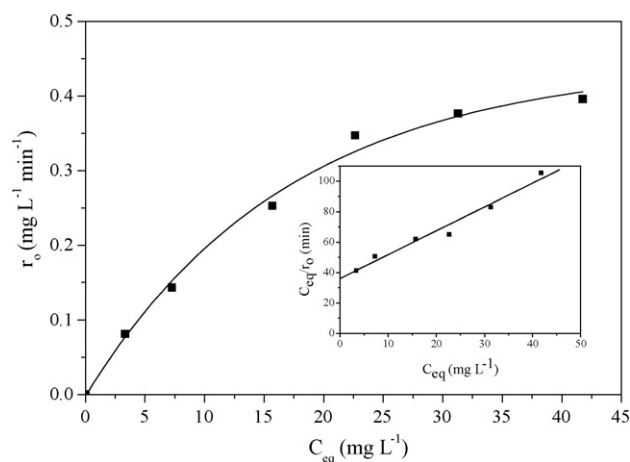
Fig. 2. Plot of r_0 vs. C_{eq}, at various initial concentrations of imidacloprid from 5 to 50 mg L^{-1} for constant concentration of TiO$_2$ P-25 at 0.5 g L^{-1}. Inset: linear transform of C_{eq}/r_0 vs. C_{eq} according to Eq. (4).

Fig. 3. Plot of the initial reaction rate, r_0 (■) and the apparent photonic efficiency ζ_0 (%) (●) of degradation vs. $C_{TiO_2 P-25}$ for 20 mg L^{-1} of imidacloprid at different concentrations of the catalyst.

equilibration in the dark, instead of the initial one (C_0), has been used in the kinetic study.

The dependence of C_{eq}/r_0 values on the respective equilibrium concentrations of imidacloprid for constant concentration of TiO$_2$ P-25 at 0.5 g L^{-1} is shown in inset of Fig. 2. From the slope and the intercept of the resulting straight line (R^2 = 0.97), k_r and K values are computed equal to 0.638 mg L^{-1} min^{-1} and 0.043 L mg^{-1}, respectively. As already mentioned, K represents the equilibrium constant for the adsorption of imidacloprid onto TiO$_2$ and k_r reflects the limiting rate of reaction at maximum coverage for the given experimental conditions and accordingly have no absolute meaning.

In order to study the effect of catalyst' initial concentration on the degradation of imidacloprid, experiments were conducted using different concentrations of TiO$_2$ P-25 in the range of 0.25–4 g L^{-1}. Fig. 3 shows the initial reaction rate, r_0 and the apparent photonic efficiency ζ_0 during the degradation of 20 mg L^{-1} imidacloprid as a function of catalyst concentration. The reaction rate is directly proportional to the amount of catalyst up to a certain value (i.e. 0.5 g L^{-1}), at the conditions in question, above which further increases do not affect the reaction rate. This threshold value depends on the geometry and the working
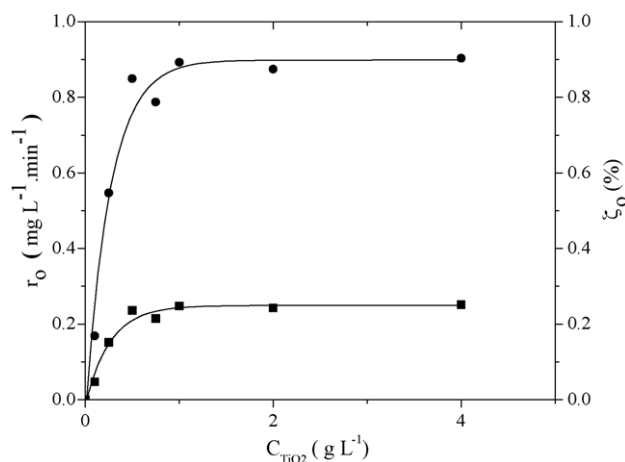
conditions of the reactor and the initial concentration of the pollutant and corresponds to the optimum of light absorption. Above this concentration, the suspended particles of the catalyst block the UV-light passage and increase the light scattering [31,32].

The addition of an electron acceptor such as H$_2$O$_2$, K$_2$S$_2$O$_8$, Fe^{3+}, Ag^{1+}, etc. to a semiconductor suspension usually enhances the photodegradation rate of organic pollutants [33,34], due to the fact that these substances capture the photogenerated electrons more effectively than dissolved oxygen, leading to a reduction of the electron-hole recombination. In this study, the effect of adding hydrogen peroxide and/or Fe^{3+} on the photocatalytic degradation of imidacloprid was evaluated. As seen from the C–t profiles in Fig. 4 and from the photonic efficiencies in Table 1, addition of 7 mg L^{-1} Fe^{3+} or 50 mg L^{-1} H$_2$O$_2$ separately to the TiO$_2$ suspension increases slightly the extent of imidacloprid degradation and has practically no effect on mineralization; however, the simultaneous use of hydrogen peroxide and iron increases considerably both the degradation and mineralization efficiencies of the insecticide in comparison to the aforementioned experiments. The fact that the addition of Fe^{3+} alone only marginally improves degradation may be associated with the relatively low iron to TiO$_2$ concentration
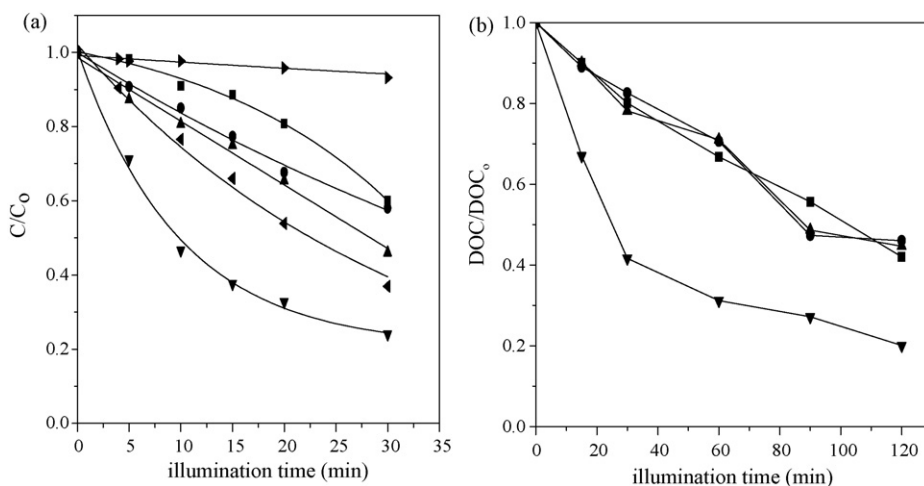
Fig. 4. Degradation (a) and mineralization (b) of 20 mg L^{-1} imidacloprid at pH 3.2 as a function of illumination time. (▶) Fe^{3+} (7 mg L^{-1}) + H$_2$O$_2$ (50 mg L^{-1}) in the dark, (■) TiO$_2$ (0.5 mg L^{-1}), (●) TiO$_2$ (0.5 mg L^{-1}) + Fe^{3+} (7 mg L^{-1}), (▲) TiO$_2$ (0.5 mg L^{-1}) + H$_2$O$_2$ (50 mg L^{-1}), (◀) Fe^{3+} (7 mg L^{-1}) + H$_2$O$_2$ (50 mg L^{-1}), and (▼) TiO$_2$ (0.5 mg L^{-1}) + Fe^{3+} (7 mg L^{-1}) + H$_2$O$_2$ (50 mg L^{-1}).

Table 1
Initial apparent photonic efficiencies of degradation (ζ_0) and mineralization (ζ_{DOC}) of 20 mg L^{-1} imidacloprid for various photocatalytic systems at pH 3.2

Run no.	Reaction system	ζ_0 (%)	ζ_{DOC} (%)
1	0.5 g L^{-1} TiO$_2$ P-25	0.66 ± 0.014	3.40 ± 0.32
2	0.5 g L^{-1} TiO$_2$ P-25 + 7 mg L^{-1} Fe^{3+}	1.06 ± 0.05	3.93 ± 0.40
3	0.5 g L^{-1} TiO$_2$ P-25 + 50 mg L^{-1} H$_2$O$_2$	1.12 ± 0.09	4.10 ± 0.43
4	0.5 g L^{-1} TiO$_2$ P-25 + 7 mg L^{-1} Fe^{3+} + 50 mg L^{-1} H$_2$O$_2$	3.64 ± 0.17	14.11 ± 3.39
5	7 mg L^{-1} Fe^{3+} + 200 mg L^{-1} H$_2$O$_2$	1.49 ± 0.02	4.98 ± 0.23
6	7 mg L^{-1} Fe^{3+} + 200 mg L^{-1} H$_2$O$_2$	0.30 ± 0.03	0.80 ± 0.14
7	7 mg L^{-1} Fe^{3+} + 200 mg L^{-1} H$_2$O$_2$ + 33 mg L^{-1} oxalate ions	4.24 ± 1.09	29.84 ± 4.99
8	7 mg L^{-1} Fe^{3+} + 200 mg L^{-1} H$_2$O$_2$ + 33 mg L^{-1} oxalate ions	2.52 ± 0.17	36.41 ± 4.37

Experiments 1–5 and 7 under UV-A and 6 and 8 under visible illumination.

ratio employed, i.e. the catalytic activity of iron is masked by that of TiO$_2$. A similar explanation was provided by Meštánková et al. [35] who studied the effect of iron on the photocatalytic degradation of monuron and found that iron contribution was more important at decreased TiO$_2$ concentrations. On the other hand, addition of 50 mg L^{-1} H$_2$O$_2$ has little effect on imidacloprid oxidation and this is also the case for runs performed at H$_2$O$_2$ concentrations up to 400 mg L^{-1}. For the ternary TiO$_2$/Fe^{3+}/H$_2$O$_2$ system, the initial reaction rate for imidacloprid degradation and mineralization calculated from the C–t data in Fig. 4 is 1.02 and 0.18 mg L^{-1} min^{-1}, respectively; these values are nearly twice as much as the sum of rates or photonic efficiencies of the individual TiO$_2$ and photo-Fenton processes under UV-A illumination, thus implying a synergistic effect. The beneficial effect arising from process coupling may be ascribed to (i) the simultaneous activation of heterogeneous and homogeneous (photo-Fenton reagent) photocatalytic oxidation and (ii) the fact that Fe^{3+} ions, which are adsorbed strongly onto the TiO$_2$ surface, are able to act as efficient electron acceptors minimizing the recombination of photogenerated carriers, as well as regenerating Fe^{2+} in a catalytic redox cycle, besides the additional light reduction of Fe^{3+} to Fe^{2+} (see also Eq. (6)), thus making the combined process more efficient than the individual systems. It should be noticed though that the combination of heterogeneous and homogeneous photocatalytic oxidation constitutes a very complex system in which several processes occur at the same time, contributing to the overall rate [36].

3.2. Homogeneous photocatalytic experiments

In recent years, the Fenton process has been extensively employed for the oxidation of many classes of organic compounds due to its high efficiency to generate hydroxyl radicals, as a result of the decomposition in acidic medium of H$_2$O$_2$ by Fe^{2+} ions [37]. This reagent is an attractive oxidative system, which produces in a very simple way OH$^\bullet$ radicals (Eq. (5)) for wastewater treatment, due to the fact that iron is a very abundant and non-toxic element and hydrogen peroxide is easy to handle and environmentally safe. A disadvantage of this process is that it requires stoichiometric amounts of Fe^{2+}. However, it was found that UV-A/vis light (artificial or natural), can made the process catalytic, by photo-reducing the Fe^{3+} to Fe^{2+}, producing additional OH$^\bullet$ radicals and leading to the regeneration of the catalyst (Eq. (6)) (photo-Fenton reaction) [38,39]. These reactions are known to be the primary forces of the photochemical self-cleaning of atmospheric and aquatic environment [40].

$$Fe^{2+} + H_2O_2 \rightarrow Fe^{3+} + OH^- + OH^\bullet \quad (5)$$

$$Fe^{3+} + H_2O + h\nu(<450\,nm) \rightarrow Fe^{2+} + H^+ + OH\cdot \quad (6)$$

The main advantage of this process is the ability of using sunlight with light sensitivity up to 450 nm, thus avoiding the high costs of UV lamps and electrical energy. The disadvantages of the process are the low pH values which are required, since iron precipitates at higher pH values and the fact that iron has to be removed after treatment.

The effect of oxidant concentration on imidacloprid degradation and mineralization during photo-Fenton/UV-A oxidation was studied and the results, in terms of initial degradation and mineralization rates, are shown in Fig. 5. As seen, the degradation rate of 20 mg L^{-1} imidacloprid increases with increasing H$_2$O$_2$ concentration up to about 50 mg L^{-1} and then remains constant at concentrations up to 200 mg L^{-1}. Nonetheless, increasing the concentration from 200 to 400 mg L^{-1} has a detrimental effect on degradation since at high concentrations hydrogen peroxide may act as a hole or OH$^\bullet$ scavenger.

Taking into account that photo-Fenton reactions may also be initiated by light from the visible part of the spectrum [41,42], experiments were conducted using an irradiation source with exactly the same geometry as the UV-A source, that emits above 400 nm. Moreover, experiments were performed in the presence of ferrioxalate, a Fe^{3+}/oxalate complex (molar ratio Fe^{3+}:oxalate ions 1–3), which is claimed to be capable of enhancing the efficiency of photo-Fenton reactions [42].

Fig. 6 shows the degradation and mineralization temporal profiles during the homogeneous photocatalytic degradation of 20 mg L^{-1} imidacloprid, while Table 1 shows the respective apparent photonic efficiencies. As seen, the ferrioxalate reagent (7 mg L^{-1} + 33 mg L^{-1} oxalate ions + 200 mg L^{-1} H$_2$O$_2$) under UV-A or visible light is faster than the respective photo-Fenton reaction (7 mg L^{-1} + 200 mg L^{-1} H$_2$O$_2$), and more importantly, has a considerably greater photonic efficiency. In all cases though, homogeneous photocatalytic reactions are more efficient than the respective heterogeneous system (i.e. TiO$_2$/UV-A) in terms of both imidacloprid degradation and mineralization. Interestingly, photo-Fenton under visible light is substantially slower (by an order of magnitude as seen in Table 1) than the respective reaction under UV-A irradiation. After 90 min of reaction, only about 40% imidacloprid conversion has been recorded under visible irradiation and this is consistent with the relatively low mineralization (i.e. 10%) recorded, possibly due to the lower light intensity (see experimental part), the decrease of the quantum yield of the hydroxyl radical/ferrous ion formation with increasing wavelength and the difficulty to break down the aromatic rings containing the heteroatoms. The respective values for the runs under UV-A light are 90 and 60%.

Fig. 5. Effect of H$_2$O$_2$ concentration on imidacloprid initial degradation and mineralization rates during photo-Fenton/UV-A oxidation at 20 mg L^{-1} imidacloprid and 7 mg L^{-1} Fe^{3+} (pH 3.2).

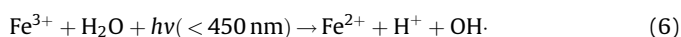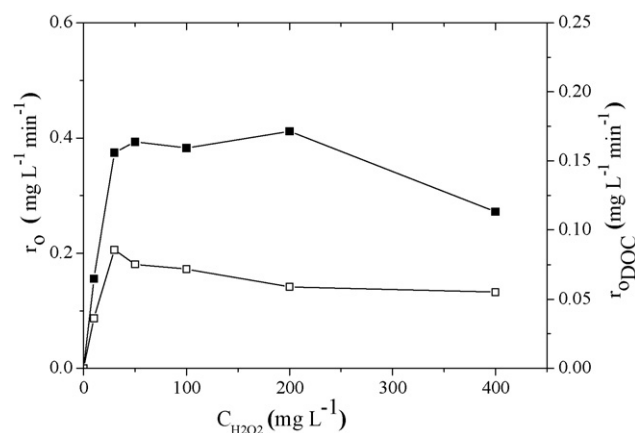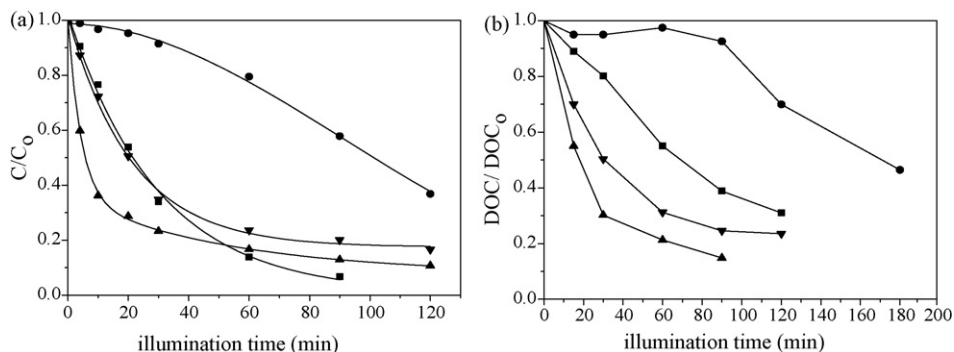**Fig. 6.** Photocatalytic degradation (a) and mineralization (b) of 20 mg L^{-1} imidacloprid at pH 3.2 as a function of illumination time. (■) photo-Fenton/UV-A, (●) photo-Fenton/vis, (▲) ferrioxalate/UV-A, and (▼) ferrioxalate/vis. H_2O_2 = 200 mg L^{-1}; Fe^{3+} = 7 mg L^{-1}; oxalate ions = 33 mg L^{-1}.

The reason for the improved performance of the ferrioxalate process is believed to be the high quantum yield of Fe^{2+} formation over a broad range of irradiation (250–500 nm) leading at least to one OH• radical for every quantum of light energy absorbed by ferrioxalate, as well as the fact that it absorbs over a broader range of wavelengths in comparison to the photo-Fenton reagent and thus utilizes the UV/vis output more efficiently [42,43].

3.3. Imidacloprid degradation by-products, reaction pathways and ecotoxicity

The photocatalytic mineralization of imidacloprid leads to the formation of various reaction intermediates, whose carbon atoms are eventually oxidized to carbon dioxide and water, while heteroatoms are converted to inorganic anions that remain in the solution, according to the following overall reaction scheme:

$$C_9H_{10}O_2N_5Cl + 16.5O_2 \xrightarrow[h\nu]{catalyst} 9CO_2 + 5HNO_3 + HCl + 2H_2O \quad (7)$$
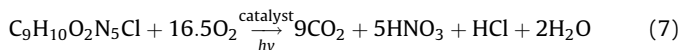
To elucidate the routes through which imidacloprid is converted to reaction by-products and eventually to end-products, besides the DOC reduction, samples subject to various experimental conditions were analyzed with respect to (i) the release of inorganic nitrogen compounds and chloride in the reaction mixture and (ii) the identification of major intermediates.
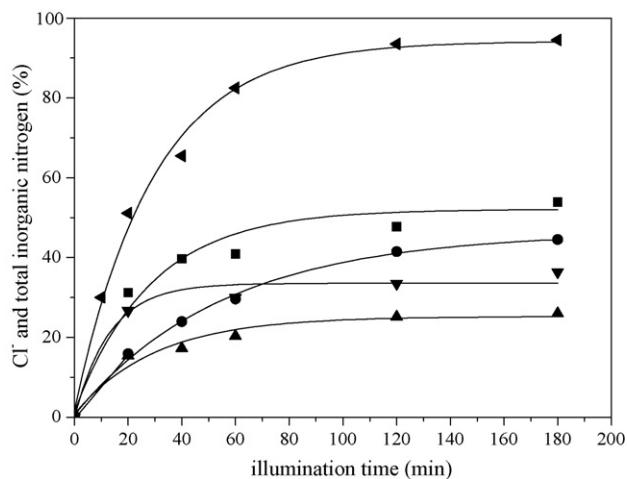

Fig. 7. Inorganic ions production during the photocatalytic degradation of 20 mg L^{-1} imidacloprid. (◄) Chloride release in the presence of 0.5 g L^{-1} TiO$_2$/UV-A. Total inorganic nitrogen as a sum of nitrogen in NH_4^+ and NO_3^-: (■) 0.5 mg L^{-1} TiO$_2$ P-25/UV-A + (7 mg L^{-1} Fe^{3+} + 200 mg L^{-1} H_2O_2), (●) photo-Fenton/UV-A (7 mg L^{-1} Fe^{3+} + 200 mg L^{-1} H_2O_2), (▼) 0.5 g L^{-1} TiO$_2$ P-25/UV-A, and (▲) photo-Fenton/vis (7 mg L^{-1} Fe^{3+} + 200 mg L^{-1} H_2O_2).

Fig. 7 shows concentration–time profiles of total inorganic nitrogen (i.e. the sum of nitrogen contained in NO_3^-, NH_4^+ and NO_2^-) as percentage of the theoretical nitrogen contained in imidacloprid for various photocatalytic systems. In all cases, ammonium and nitrate were the dominant inorganic nitrogen species formed during the photocatalytic degradation of imidacloprid, while only trace amounts of NO_2^- were detected which, upon prolonged irradiation, they were oxidized to NO_3^-. After 180 min of illumination, the NH_4^+/NO_3^- ratio was, in all cases, nearly equimolar. Under the given experimental conditions the conversion of the organic nitrogen to inorganic ions is a relatively inefficient process ranging between about 30% for the photo-Fenton/UV-A to 50% for the combined TiO$_2$/Fe^{3+}/H$_2O_2$ system, thus implying that other nitrogen-containing organic compounds (various aliphatic amines or amides after ring opening) are present in the solution. However, as seen from Figs. 4, 6 and 7 the relative efficiency of various processes for mineralization matches that for nitrogen conversion. A possible explanation for the reduced conversion of organic nitrogen to inorganic ions may be the relatively low irradiation intensity and short illumination time employed, as well as the low oxidation state of nitrogen in imidacloprid, all of which are known to affect the final oxidation state of nitrogen in photocatalytic reactions [44,45].

Fig. 7 also shows the concentration–time profile of chloride anion release (as percentage of the theoretical chlorine contained in imidacloprid) for the TiO$_2$/UV-A system. Chlorine is easily transformed to its anion and nearly complete dechlorination can be achieved after 120 min of reaction.

To determine reaction by-products accompanying imidacloprid photocatalytic oxidation, samples of the experiments shown in Fig. 7 were analyzed by means of GC/MS. As seen in Table 2, three ring (1–3) and five linear (4–8) compounds were successfully

Table 2
Reaction by-products (compound numbers as in text and Fig. 8) detected in samples subject to various treatment conditions as in Fig. 8

Compound number	Photo-Fenton/ UV-A		Photo-Fenton/vis		TiO$_2$/UV-A	
	30 min	60 min	30 min	60 min	30 min	60 min
1	nd	nd	nd	nd	●	nd
2	nd	nd	nd	nd	●	nd
3	nd	nd	nd	nd	●	●
4	nd	●	nd	nd	nd	●
5	nd	nd	nd	nd	nd	●
6	●	●	nd	nd	nd	nd
7	nd	●	●	nd	nd	nd
8	nd	nd	●	nd	nd	nd

nd: not detected.

detected, namely: 6-chloronicotic acid (1), 1-(6-chloro-3-pyridi-nyl)methyl-2-imidazolidinone (2), methyl-6-chloronicotinate (3), N-ethylformamide (4), 2-methyl-1-nitropropane (5), dimethyl formamide (6), amyl nitrite (7) and chlorine dioxide (8) with numbers in brackets corresponding to their structures as shown in Fig. 8. The reason that some of the identified compounds do not appear in certain treatment schemes of Table 2 is most likely due to the use of different operating conditions rather than the involvement of substantially dissimilar reaction mechanisms. This is so, since the mechanisms upon which all the aforementioned processes rely, basically involve the formation and participation of reactive moieties such as hydroxyl radicals, in order to promote the degradation of organics via redox reactions.

It can be safely assumed, that 6-chloronicotic acid and 1-(6-chloro-3-pyridinyl)methyl-2-imidazolidinone are early-stage degradation by-products that are formed as follows: imidacloprid converts to 6-chloronicotic aldehyde (a compound which was not detected possibly due to its reactivity) which is then oxidized to the respective acid. Moreover, removal of imidacloprid nitro group and subsequent oxidation at the imidazolidine ring leads to the formation of 1-(6-chloro-3-pyridinyl)methyl-2-imidazolidinone. Both routes shown in Fig. 8, have been also proposed in earlier studies dealing with imidacloprid degradation by means of solar TiO_2 photocatalysis [46,47], solar photo-Fenton [47] and UV-A photolysis [48]. In a recent work [49], the photoinduced degradation of imidacloprid was studied in natural water samples

Fig. 8. Structures of imidacloprid and identified by-products formed during the photocatalytic degradation.
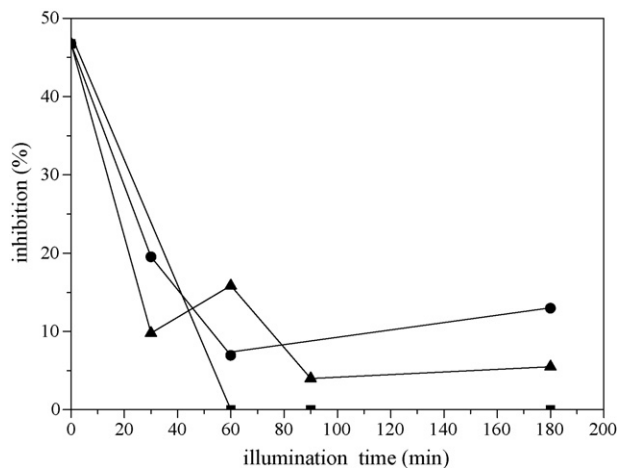
Fig. 9. Change of ecotoxicity of imidacloprid (20 mg L^{-1} initial concentration) as a function of illumination time for various treatments. (■) TiO$_2$ P-25 (0.5 g L^{-1}), (●) photo-Fenton/UV-A (7 mg L^{-1} Fe^{3+} + 200 mg L^{-1} H$_2$O$_2$), and (▲) photo-Fenton/vis (7 mg L^{-1} Fe^{3+} + 200 mg L^{-1} H$_2$O$_2$).

and several ring by-products were identified including, among others, 1-(6-chloro-3-pyridinyl)methyl-2-imidazolidinone and methyl-6-chloronicotinate. As soon as the ring cleavage occurs, several linear compounds are formed some of which were successfully identified. It should be pointed out that, other than the compounds successfully detected, several other chromatographic peaks were also found but could not be positively identified (i.e. the match factor of the mass spectrum was below 90%).

Fig. 9 shows changes in imidacloprid acute ecotoxicity to *V. fischeri* (exposure time of 15 min) as a function of treatment time for various photocatalytic processes. Imidacloprid at 20 mg L^{-1} initial concentration is strongly toxic with inhibition being as high as 50%. However, following treatment ecotoxicity either decreases substantially (i.e. for the samples subject to photo-Fenton oxidation) or is completely eliminated (for the sample subject to TiO$_2$ photocatalysis) implying that degradation intermediates are less ecotoxic than the original substrate itself. It should be pointed out that for photo-Fenton oxidation runs, the remaining toxicity cannot be attributed to residual, unreacted hydrogen peroxide (a well-known disinfectant) as this was removed prior to analysis. These results are in agreement with those reported by Segura et al. [50] and Malato et al. [47] who reported that imidacloprid acute ecotoxicity to *Daphnia magna* progressively decreased upon (i) photo-Fenton oxidation induced by UV-A fluorescent lamps or natural sunlight and (ii) TiO$_2$ solar photocatalysis [46].

4. Conclusions

In this work, the photocatalytic degradation and mineralization of imidacloprid, a systemic chloronicotinoid insecticide, has been investigated. TiO$_2$ heterogeneous photocatalysis under UV-A irradiation is a relatively slow process with quantitative degradation of imidacloprid occurring in more than 240 min of reaction. Coupling TiO$_2$ with Fe^{3+} or H$_2$O$_2$ separately has little effect on degradation efficiency; however, the simultaneous use of TiO$_2$, Fe^{3+} and H$_2$O$_2$ leads to significantly increased rates presumably due to the combined effects of homogeneous and heterogeneous photocatalytic reactions. This is accompanied by quantitative dechlorination, partial conversion of organic nitrogen to inorganic species and increased but incomplete mineralization, thus implying the formation of stable reaction by-products; several of these were successfully identified.

The photo-Fenton process based on UV-A or visible light was considerably faster than heterogeneous photocatalysis and its efficiency improved further coupling photo-Fenton reagents with the oxalate ion.

From the results of the present work and the respective literature, one could claim that both photocatalytic methods could be employed as powerful tools for the elimination of this class of materials. The use of catalysts such as TiO$_2$ or Fe^{3+} and the possibility of their activation with UV-A, vis or solar light (which is not the case in most advanced oxidation technologies), combined with the simple technology required for these methods, can offer economically reasonable and practical solutions to the processing of this type of pollutants. Nonetheless, the drawbacks of either process should carefully be taken into account prior to the selection of a treatment scheme. For instance, homogeneous photocatalysis requires operation at controlled pH conditions and the need to remove iron ions from the treated solution; in this respect, additional treatment stages are needed, thus increasing treatment costs. Likewise, heterogeneous photocatalysis with suspended TiO$_2$ would also require an additional step to remove solid particles from the liquid phase. The need to remove the photocatalyst from the liquid phase can be avoided though using immobilized rather than suspended configurations. In either process, the use of H$_2$O$_2$ as an additional source of hydroxyl radicals is indeed beneficial in terms of increased treatment efficiency but it is also expected to increase treatment costs.

References

[1] S.C. Nixon, T.J. Lack, D.T.E. Hunt, A.F. Boschet, Sustainable use of Europe's water? State, prospects and issues, European Environmental Agency, Environmental Assessment Series No. 7, 2000.
[2] A.N. Angelakis, M.H.F. Marekos, L. Bontoux, T. Asano, Water Res. 33 (1999) 2201–2217.
[3] J.W. Readman, T. Albanis, D. Barcelo, S. Galassi, J. Tronczynski, G. Gabrielides, Mar. Pollut. Bull. 26 (1993) 613–619.
[4] D.W. Kopling, E.M. Thurman, D.A. Goosby, Environ. Sci. Technol. 30 (1996) 335–340.
[5] M.T. Meyer, E.M. Thurman, Herbicide Metabolites in Surface Water and Ground Water, ACS Symposium Series 630, American Chemical Society, Washington, DC, 1996.
[6] M.G. Hayo, Agric. Ecosyst. Environ. 60 (1996) 81–96.
[7] J. Blanco, S. Malato, Solar detoxification. UNESCO, Natural Sciences, World Solar Programme 1996–2005 [chapter 2], ⟨http://www.unesco.org/science/wsp⟩, 2001.
[8] P.J. Robertson, D.W. Bahnemann, J.M.C. Robertson, F. Wood, Handbook of Environmental Chemistry, vol. 2, Part M, Springer-Verlag, Berlin, Heidelberg, 2005, pp. 367–423.
[9] D. Blake, Bibliographic work on the heterogeneous photocatalytic removal of hazardous compounds from water and air, National Renewable Energy Laboratory, Technical Report, NREL/TP-510-31319, 2001.
[10] I.K. Konstantinou, T.A. Albanis, Appl. Catal. B 42 (2003) 319–335.
[11] R.R. Ishiki, H.M. Ishiki, K. Takashima, Chemosphere 58 (2005) 1461–1469.
[12] P.L. Huston, J.J. Pignatello, Water Res. 33 (1999) 1238–1246.
[13] B. Toepfer, A. Gora, G. Li Puma, Appl. Catal. B 68 (2006) 171–180.
[14] A. Elbert, B. Becker, J. Hartwig, C. Erdelen, Pflanzenschutz-Nachr. 44 (1991) 113–136.
[15] F. Krämer, N. Mencke, Flea Biology and Control: The Biology of the Cat Flea, Control and Prevention with Imidacloprid in Small Animals, Springer-Verlag, Berlin, Heidelberg, New York, 2001.
[16] A.M. Braun, M. Maurette, E. Oliveros, Photochemical Technology, Wiley, New York, 1991.
[17] E. Psillakis, A. Ntelekos, D. Mantzavinos, E. Nikolopoulos, N. Kalogerakis, J. Environ. Monit. 5 (2003) 135–140.
[18] T. Velegraki, I. Poulios, M. Charalabaki, N. Kalogerakis, P. Samaras, D. Mantzavinos, Appl. Catal. B 62 (2006) 159–168.
[19] C. Berberidou, I. Poulios, N.P. Xekoukoulotakis, D. Mantzavinos, Appl. Catal. B 74 (2007) 63–72.
[20] M. Muneer, D. Bahnemann, Appl. Catal. B 36 (2002) 95–111.
[21] A. Chatzitakis, C. Berberidou, I. Paspaltsis, G. Kyriakou, T. Sklaviadis, I. Poulios, Water Res. 42 (2008) 386–394.
[22] M.R. Hoffman, S. Martin, W. Choi, D. Bahnemann, Chem. Rev. 95 (1995) 69–96.
[23] A. Fujishima, T.N. Rao, D.A. Tryk, J. Photochem. Photobiol. C 1 (2000) 1–21.
[24] J.B. Baxter, C.A. Schmuttenmaer, J. Phys. Chem. B 110 (2006) 25229–25239.
[25] E.A. Meulenkamp, J. Phys. Chem. B 103 (1999) 7831–7838.

[26] P. Spathis, I. Poulios, Corros. Sci. 37 (1995) 673–680.
[27] M. Kositzi, I. Poulios, K. Samara, E. Tsatsaroni, E. Darakas, J. Hazard. Mater. 146 (2007) 680–685.
[28] I. Kaiser, I. Palabrica, Water Pol. Res. J. Can. 26 (1991) 361–431.
[29] J. Cunningham, G. Al-Sayyed, S. Srijaranai, in: G. Helz, R. Zepp, D. Crosby (Eds.), Aquatic and Surface Photochemistry, Lewis Publishers, CRC Press, 1994, pp. 317–348 (Chapter 22).
[30] H. Al-Ekabi, N. Serpone, J. Phys. Chem. 92 (1988) 5726–5731.
[31] S. Parra, J. Olivero, C. Pulgarin, Appl. Catal. B 36 (2002) 75.
[32] S. Kaniou, K. Pitarakis, I. Barlagianni, I. Poulios, Chemosphere 60 (2005) 372–380.
[33] E.J. Wolfrum, D.F. Ollis, in Ref. [29], chapter 32, 451–465.
[34] S. Malato, J. Blanco, M.I. Maldonado, P. Fernandez-Ibanez, A. Campos, Appl. Catal. B 28 (2000) 163–174.
[35] H. Meštánková, J. Krýsa, J. Jirkovský, G. Mailhot, M. Bolte, Appl. Catal. B 58 (2005) 185–191.
[36] N. Quici, M.E. Morgada, R.T. Gettar, M. Bolte, M.I. Litter, Appl. Catal. B 71 (2007) 117–124.
[37] E. Neyens, J. Baeyens, J. Hazard. Mater. 98 (2003) 33–50.
[38] E. Oliveros, O. Legrini, M. Hohl, T. Mueller, A. Braun, Chem. Eng. Process. 36 (1997) 397–405.
[39] H. Fallmann, T. Krutzler, R. Bauer, S. Malato, J. Blanco, Catal. Today 54 (1999) 309–319.
[40] B.C. Faust, R.G. Zepp, Environ. Sci. Technol. 27 (1993) 2517–2522.
[41] G. Ruppert, R. Bauer, G.J. Heisler, J. Photochem. Photobiol. A 73 (1993) 75–78.
[42] A. Safarzadeh-Amiri, J. Bolton, S. Catter, Water Res. 31 (1997) 787–798.
[43] K.A. Hislop, J.R. Bolton, Environ. Sci. Technol. 33 (1999) 3119–3126.
[44] G.K.C. Low, S.R. McEvoy, R.W. Matthews, Environ. Sci. Technol. 25 (1991) 460–467.
[45] P. Calza, E. Pelizzetti, C. Minero, J. Appl. Electrochem. 35 (2005) 665–673.
[46] S. Malato, J. Caceres, A. Aguera, M. Mezcua, D. Hernando, J. Vial, A.R. Fernandez-Alba, Environ. Sci. Technol. 35 (2001) 4359–4366.
[47] A. Aguera, E. Almansa, S. Malato, M.I. Maldonado, A.R. Fernandez-Alba, Analusis 26 (1998) 245–251.
[48] H. Wamhoff, V. Schneider, J. Agr. Food Chem. 47 (1999) 1730–1734.
[49] D. Redlich, N. Shahin, P. Ekici, A. Friess, H. Parlar, Clean 35 (2007) 452–458.
[50] C. Segura, C. Zaror, H.D. Mansilla, M. Angelica Mondaca, J. Hazard. Mater. 150 (2008) 679–686.